ARMA 22–0234

Strength of Utah Coal Evaluated Using Laboratory Tests with an Unloading Path

Walton, G.
Colorado School of Mines, Golden, Colorado, United States
Kim, B.H. and Larson, M.K.
CDC NIOSH, Spokane, Washington, United States

This paper was prepared for presentation at the 56th US Rock Mechanics/Geomechanics Symposium held in Santa Fe, New Mexico, USA, 26-29 June 2022. This paper was selected for presentation at the symposium by an ARMA Technical Program Committee based on a technical and critical review of the paper by a minimum of two technical reviewers. The material, as presented, does not necessarily reflect any position of ARMA, its officers, or members. Electronic reproduction, distribution, or storage of any part of this paper for commercial purposes without the written consent of ARMA is prohibited. Permission to reproduce in print is restricted to an abstract of not more than 200 words; illustrations may not be copied. The abstract must contain conspicuous acknowledgement of where and by whom the paper was presented.

ABSTRACT: Conventional triaxial tests evaluate rock strength using a load path where the minimum principal stress is held constant and the maximum principal stress is increased monotonically until the peak strength is achieved. Although brittle rock mechanical behavior is relatively well-understood under this loading path, in many practical rock mechanics applications, damage and failure develop as a result of loss of confinement (decreasing minimum principal stress). Since the inelastic behavior associated with damage that develops prior to rock failure is not path-independent, it is possible that rock damage and strength characteristics may differ depending on the loading path considered. To investigate this potential path-dependence, a series of tests were performed on Utah Coal where, following attainment of a target confining stress and deviatoric stress, the confining stress was decreased at a constant rate until failure while maintaining the deviatoric stress. These results were then compared to previously published data for Utah Coal obtained using conventional laboratory testing procedures. The previously published data for Utah Coal showed highly confinement-dependent strength behavior, where the peak strength increased by as much as up to 50% of the mean unconfined compressive strength (UCS) with confining stresses as low as 1% of the UCS applied. The peak strength and crack damage (CD) envelopes were found to be highly anisotropic, but the crack initiation (CI) envelope was relatively insensitive to the angle between the loading direction and the primary cleat orientation. In this study, although the CI stress, CD stress, and peak strength envelopes are all generally similar for both the loading and unloading tests, some of the test results for samples with cleating inclined at 30° to the loading direction suggest the CD stress envelope may be slightly lower under unloading conditions than under loading conditions.

1. INTRODUCTION

Standard methods for determination of the strength of rock under compression follow a loading path, where failure is induced by monotonically increasing the major principal stress, σ_1. However, this stress path is not necessarily reflective of the stress path experienced by rock in many practical rock engineering scenarios (Martin, 1997; Kaiser et al., 2001; Eberhardt, 2001; Diederichs et al., 2004). For example, in the context of excavation development, damage is induced by a reduction in the minor principal stress (also called confining stress), σ_3. Accordingly, many authors have conducted experimental research to evaluate the compression strength of rock when an unloading stress path is used. This can be achieved using a diagonal stress path where σ_3 is decreased and σ_1 are increased simultaneously (e.g. Huang et al., 2000; Li et al., 2017), a horizontal stress path where σ_3 is decreased and σ_1 is held constant (e.g. Petitt et al., 1998; Wang et al., 2019), a rockburst testing approach where the confining stress on one face of cubic specimen loaded in a true triaxial testing machine is suddenly released (e.g. He et al., 2010; Zhao et al., 2014), or a constant deviatoric stress path where σ_3 and σ_1 are decreased at identical rates such that the failure envelope is approached along a constant deviatoric stress diagonal line in principal stress space (e.g. Xie & He, 2004). We argue that to isolate the potential impacts of stress path on strength, the use of constant deviatoric stress path unloading test is the most promising approach as it both ensures failure is driven solely by confining stress unloading (as opposed to increases in deviatoric stress) and corresponds to an unloading stress path orientation that is further from the stress path orientation of a standard triaxial test than other common unloading test stress paths.

In this study, we present the results of a series of constant deviatoric stress unloading triaxial tests conducted on Utah Coal. This rock has previously been studied in detail using standard compression tests (Kim et al., 2018; Kim et al., 2021), which allows us to make comparisons between the peak strength and damage thresholds obtained using loading and unloading paths.

2. METHODS

A total of 19 constant deviatoric stress unloading triaxial tests were conducted for this study, including 9 tests on specimens loaded with an included angle (angle between the coal's cleat plane and the direction of loading) of 0° and 10 tests on specimens loaded with an including angle of 30°. The tests were conducted at Montana Tech in Butte, Montana, using a TerraTek Model FX-S-33090 closed-loop digital servo controlled load frame. Specimens were prepared according to the relevant ASTM standard (D 4543-08). Axial displacement was recorded with two Linear Variable Displacement Transducers (LVDTs), and a TerraTek radial cantilever transducer was used to track lateral deformation.

A representative example of one of the unloading test stress paths is shown in Figure 1. The stress path for each test consisted of three component stages. First, σ_3 and σ_1 were increased simultaneously at a rate of 0.25 MPa/s until a target value of σ_3 ($\sigma_{3\text{-target}}$) was achieved. Next, σ_1 was increased at a rate of 0.0345 MPa/s until a value of σ_1 corresponding to the target deviatoric stress ($\sigma_{1\text{-target}}$) was achieved. Finally, both σ_3 and σ_1 were decreased simultaneously at a rate of 0.0345 MPa/s until specimen failure occurred.

The values of $\sigma_{3\text{-target}}$ were selected based on the UCS values for the 0° and 30° included angles for Utah Coal as estimated based on previous testing activities. Multiple different values of $\sigma_{3\text{-target}}$ and $\sigma_{1\text{-target}}$ were tested to identify combinations that would result in failure during unloading. Ultimately, it was determined that the values of $\sigma_{3\text{-target}}$ should be approximately twice the mean UCS value for the 0° included angle case and approximately three times the mean UCS value for the 30° included angle case. The values of $\sigma_{3\text{-target}}$ were set as 66 MPa and 40 MPa for the 0° and 30° included angle tests, respectively, which ensured sufficient confinement was applied to the specimens such that no damage developed during the phase of increasing deviatoric stress prior to unloading. Multiple values of $\sigma_{1\text{-target}}$ were tested for each included angle case (specific conditions considered are summarized in Table 1) with the goal of the stress paths hitting the peak strength envelope at a variety of different confining stress; 2-3 tests were run for each value of $\sigma_{1\text{-target}}$.

In addition to evaluating peak strength, the pre-peak damage stress thresholds Crack Initiation (CI) and Crack Damage (CD) were interpreted for each of the tests. Specifically, CI was determined as the first point of non-linearity where the axial stress – lateral strain curve deviated from the linear elastic trend during unloading, and CD was determined as the point of non-linearity in the axial stress-strain curve. To aid in the interpretation of these points, the lateral and axial tangent modulus values were calculated and plotted, where the first deviation from a constant lateral tangent modulus corresponds to CI and the first deviation from a constant axial tangent modulus corresponds to CD.

Table 1. Summary of test parameters considered in this study

Included angle (deg)	$\sigma_{3\text{-target}}$ (MPa)	$\sigma_{1\text{-target}}$ (MPa)
0	66	106.0
		109.9
		113.3
		114.1
30	40	56.4
		57.0
		63.3
		66.1

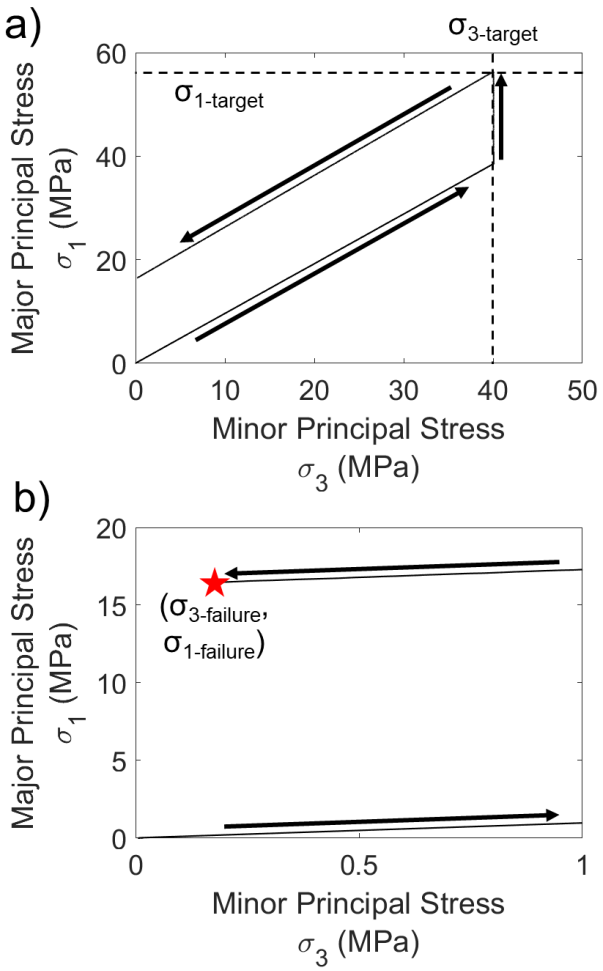

Fig. 1. Example constant deviatoric stress unloading triaxial test stress path showing (a) the full stress path and (b) a zoomed view of the start and end of the test.

3. RESULTS & DISCUSSION

Figure 2 shows a representative set of stress-strain curves from one of the unloading tests conducted for a 30° included angle specimen (the curves look similar for

the 0° included angle specimens as well). The full axial stress-strain curve shown in Figure 2a illustrates four phases of deformation: (1) crack closure during initial loading; (2) elastic deformation during initial loading; (3) elastic deformation due to increasing deviatoric stress; (4) decreasing strain due to unloading. The same four phases can be identified in the axial stress – lateral strain curve shown in Figure 2c. Note that aside from the initial crack closure phase, the remainder of the data correspond to linear segments prior to the final unloading phase, indicating that no damage was induced in the specimens prior to the start of unloading.

Figure 2b presents a zoomed view of the axial stress-strain curve during the unloading phase of the test. As unloading begins, following a brief adjustment period (the "roll-over" in the curve) the specimen begins to expand both axially and laterally in an elastic manner, corresponding to a linear portion of the stress-strain curve. As unloading continues, however, the stress path crosses the CI envelope, and distributed damage begins to develop in the specimen (Diederichs, 2003); the opening of cracks during this part of the test causes the lateral strain curve to become non-linear (Figure 2c). When the CD envelope is crossed with further unloading, the cracks begin to interact, and the apparent "stiffness" of the rock begins to decrease (Diederichs, 2003). For the servo-controlled testing machine to maintain the desired rate of unloading without allowing excess unloading to occur due to specimen damage, the rate at which axial strain decreases must correspondingly get smaller (i.e. the rate at which the ram backs off the specimen slows). This results in the axial stress-strain curve deviating from linearity (around σ_1 = 32 MPa in Figure 2b). As damage continues to accumulate in the specimen, the degree to which axial strain must increase relative to the linear elastic unloading line continues to accelerate. At a point shortly prior to failure, the damage in the specimen is sufficiently severe that the axial strain must begin to increase to maintain desired unloading rate (i.e. to avoid excessive unloading associated with continued damage). Ultimately, the specimen fails violently at the point where the testing system can no longer control the deformation of the specimen in a stable manner.

Figure 3 presents the peak strength data obtained from the unloading tests conducted for this study and compares them to the previously published peak strength data obtained using standard compression tests (Kim et al., 2018; Kim et al., 2021). These results indicate that for both included angles tested, the peak strengths obtained using an unloading stress path are functionally equivalent to those obtained using a loading stress path. No discernable differences can be seen, especially relative to the variability present in the data.

In addition to the peak strength results, trends in the CI and CD damage thresholds were evaluated. Figure 4 shows representative tangent modulus plots used for the interpretation of CI and CD. Note that unlike in a standard triaxial test conducted using a monotonically increasing load up to the point of peak strength, the tangent Young's modulus during unloading increases following CD; this corresponds to the need for the rate of axial contraction to begin to decrease following CD to counteract the tendency for stress to decrease due to damage accumulation, as discussed above.

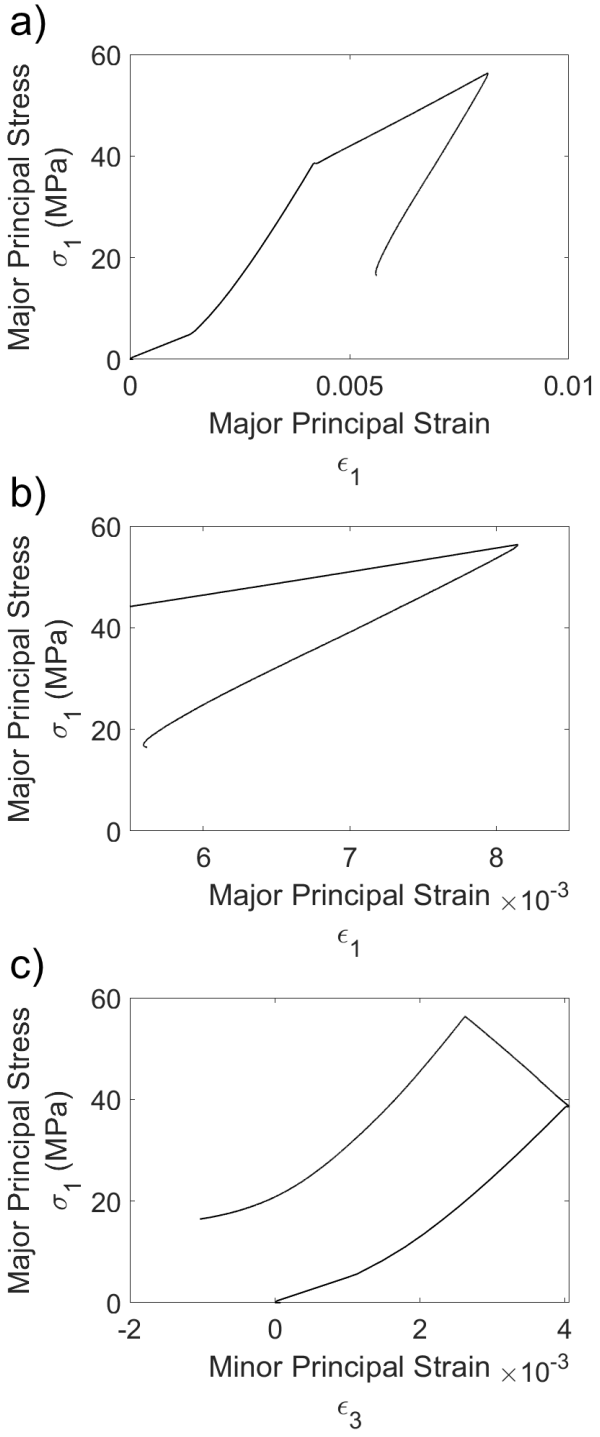

Fig. 2. Stress-strain curves for a 30° included angle specimen showing representative trends in (a) axial stress – axial strain; (b) axial stress – axial strain specifically during the unloading portion of the test; (c) axial stress – lateral strain.

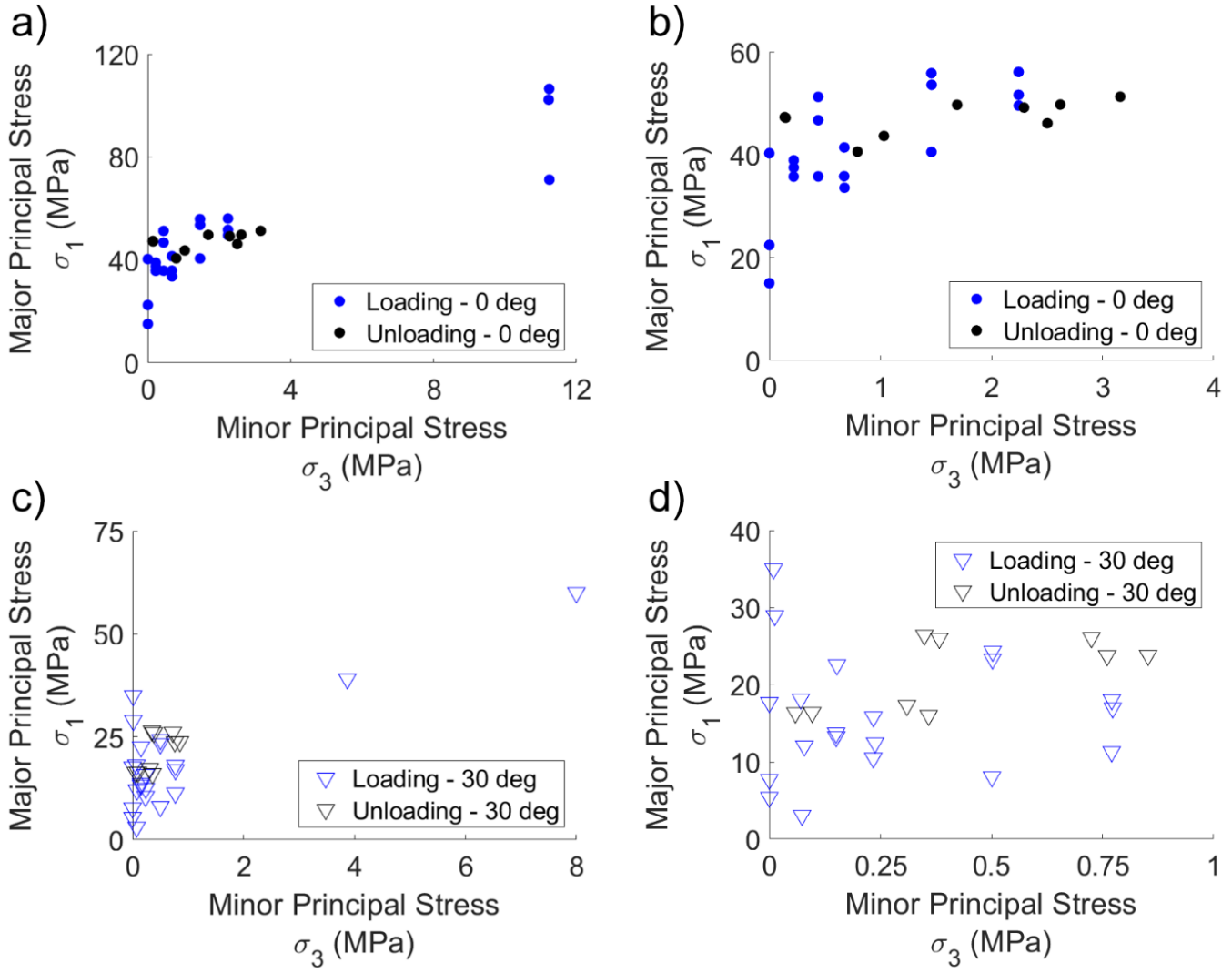

Fig. 3. Peak (failure) strength data for loading and unloading cases. (a) and (b) show data for the 0° included angle specimens (un-zoomed and zoomed views, respectively); (c) and (d) show data for the 30° included angle specimens (un-zoomed and zoomed views, respectively).

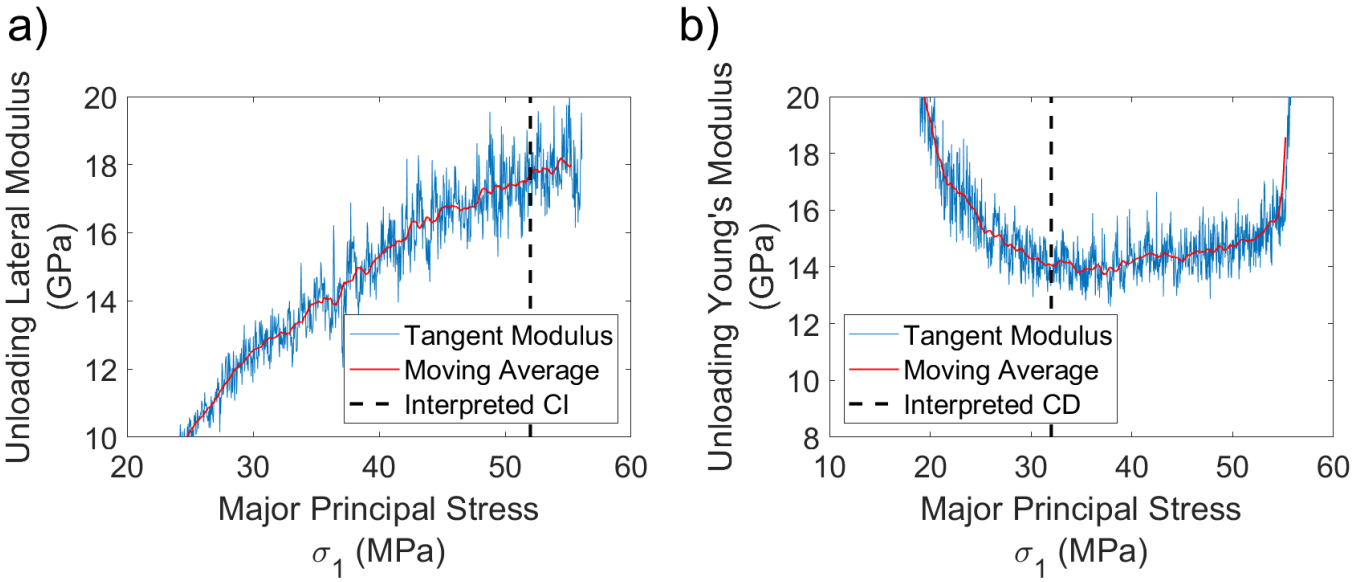

Fig. 4. Examples of determination of (a) CI and (b) CD during the unloading phase of testing.

Figure 5 shows the CI and CD results interpretated using the data from the unloading tests conducted for this study. For each included angle case, the CI values occur to the right of the CD values (higher confinement, earlier during unloading). Similar to the peak strength results, the damage thresholds for the 30° included angle case fall below those for the 0° included angle case.

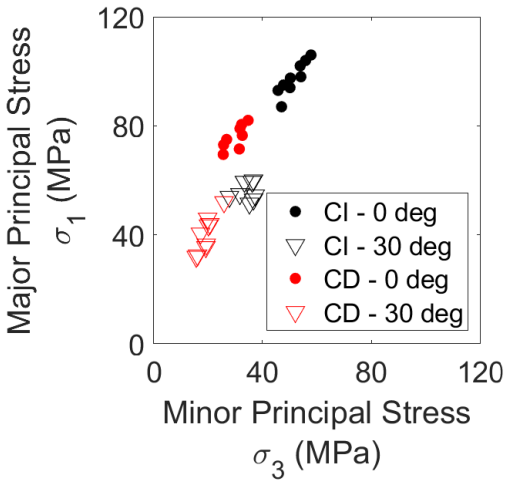

Fig. 5. Comparison of CI and CD values obtained during unloading; the linear trends present in the data correspond to the constant deviatoric stress lines followed during the unloading phase of testing.

Figure 6 presents the CI and CD results obtained from the unloading tests conducted for this study and compares them to the previously published CI and CD values data obtained using standard compression tests (Kim et al., 2018; Kim et al., 2021). These results illustrate that the CI and CD values obtained under unloading conditions are generally comparable to those obtained under loading conditions. Although the CI values obtained from the unloading tests for the 0° inclined angle specimens fall above the values obtained from several of the corresponding loading tests, their trend roughly lines up with one of the higher CI values observed under loading conditions at low confinement. Similarly, although the CD results presented in Figure 6b suggest that the 30° included angle CD trend under unloading conditions may be slightly lower than the corresponding trend for loading conditions, any such difference is small relative to the variability present in the data.

Although the results suggest that there are no significant differences in the peak strength or damage threshold envelopes when approached using a constant σ_3 loading stress path or constant deviatoric stress unloading stress path, this interpretation is somewhat inconclusive because of the relatively large degree of variability present in the data. Additionally, there are a number of factors that may have impacted the results that future study is required to evaluate, including potential influences of unloading rate and time-dependent damage effects given the relatively long test times (approximately 1 hour) required to run the unloading tests at the unloading rate considered in this study (0.0345 MPa/s).

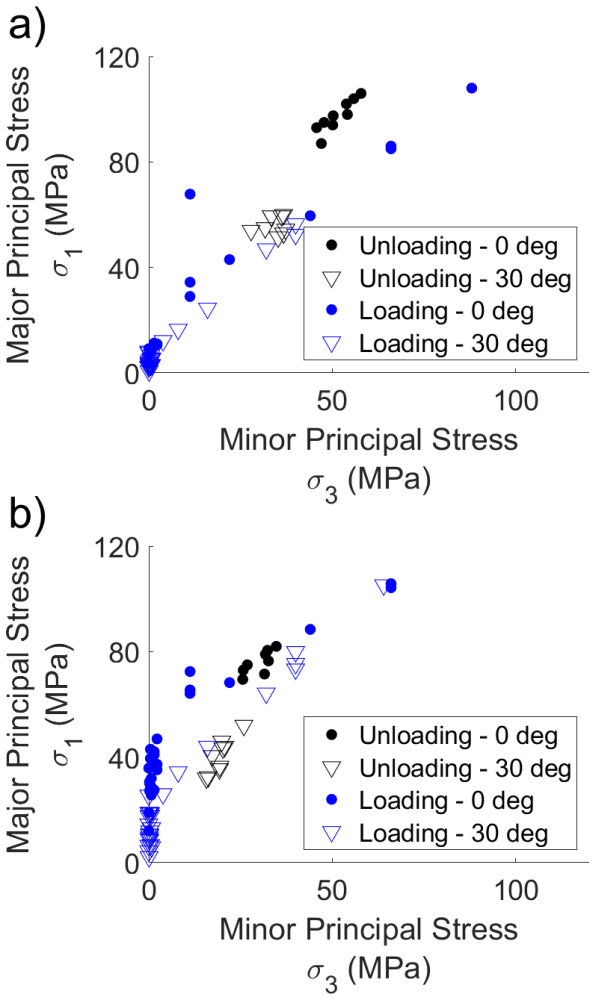

Fig. 6. Comparisons of (a) CI and (b) CD values obtained during the unloading phase of constant deviatoric stress unloading triaxial tests with those obtained from standard triaxial tests (see Kim et al., 2021).

4. CONCLUSIONS

This study presented the results of a series of triaxial compression strength tests conducted on Utah Coal using a constant deviatoric stress unloading stress path. The results showed that the peak strength envelope, crack initiation stress threshold envelope, and crack damage stress envelope for the specimens tested under unloading conditions were not significantly different from those obtained from specimens previously tested under loading conditions. However, future studies should be performed to evaluate whether this finding holds for other rock types that exhibit less variability, as well as to evaluate the influences of factors not explicitly considered in this study (such as unloading rate) on rock mechanical behavior under unloading conditions.

5. ACKNOWLEDGEMENTS

Steve Berry of Montana Tech prepared the specimens for testing and conducted the tests for this study.

6. DISCLAIMER

The findings and conclusions in this document are those of the authors and do not necessarily represent the official position of the National Institute for Occupational Safety and Health. Mention of any company or product does not constitute endorsement by NIOSH.

REFERENCES

1. Diederichs, M. S. (2003). Manuel rocha medal recipient rock fracture and collapse under low confinement conditions. *Rock Mechanics and Rock Engineering*, 36(5), 339-381.
2. Diederichs, M. S., Kaiser, P. K., & Eberhardt, E. (2004). Damage initiation and propagation in hard rock during tunnelling and the influence of near-face stress rotation. *International Journal of Rock Mechanics and Mining Sciences*, 41(5), 785-812.
3. Eberhardt, E. (2001). Numerical modelling of three-dimension stress rotation ahead of an advancing tunnel face. *International Journal of Rock Mechanics and Mining Sciences*, 38(4), 499-518.
4. He, M. C., Miao, J. L., & Feng, J. L. (2010). Rock burst process of limestone and its acoustic emission characteristics under true-triaxial unloading conditions. *International Journal of Rock Mechanics and Mining Sciences*, 47(2), 286-298.
5. Huang, R. Q., Wang, X. N., & Chan, L. S. (2001). Triaxial unloading test of rocks and its implication for rock burst. *Bulletin of Engineering Geology and the Environment*, 60(1), 37-41.
6. Kaiser, P. K., Yazici, S., & Maloney, S. (2001). Mining-induced stress change and consequences of stress path on excavation stability—a case study. *International Journal of Rock Mechanics and Mining Sciences*, 38(2), 167-180.
7. Kim, B. H., Walton, G., Larson, M. K., & Berry, S. (2018). Experimental study on the confinement-dependent characteristics of a Utah coal considering the anisotropy by cleats. *International Journal of Rock Mechanics and Mining Sciences*, 105, 182-191.
8. Kim, B. H., Walton, G., Larson, M. K., & Berry, S. (2021). Investigation of the anisotropic confinement-dependent brittleness of a Utah coal. *International Journal of Coal Science & Technology*, 8(2), 274-290.
9. Li, D., Sun, Z., Xie, T., Li, X., & Ranjith, P. G. (2017). Energy evolution characteristics of hard rock during triaxial failure with different loading and unloading paths. *Engineering Geology*, 228, 270-281.
10. Martin, C. D. (1997). Seventeenth Canadian geotechnical colloquium: the effect of cohesion loss and stress path on brittle rock strength. *Canadian Geotechnical Journal*, 34(5), 698-725.
11. Pettitt, W. S., Young, R. P., & Marsden, J. R. (1998, July). Investigating the mechanics of microcrack damage induced under true-triaxial unloading. In *SPE/ISRM rock mechanics in petroleum engineering*. OnePetro.
12. Wang, S., Wang, H., Xu, W., & Qian, W. (2019). Investigation on mechanical behaviour of dacite under loading and unloading conditions. *Géotechnique Letters*, 9(2), 130-135.
13. Xie, H. Q., & He, C. H. (2004). Study of the unloading characteristics of a rock mass using the triaxial test and damage mechanics. *International Journal of Rock Mechanics and Mining Sciences*, 41, 74-80.
14. Zhao, X. G., Wang, J., Cai, M., Cheng, C., Ma, L. K., Su, R., ... & Li, D. J. (2014). Influence of unloading rate on the strainburst characteristics of Beishan granite under true-triaxial unloading conditions. *Rock Mechanics and Rock Engineering*, 47(2), 467-483.